Article:
Zhou, D, Zhao, Y, Kotecha, A et al. (7 more authors) (2019) Unexpected mode of engagement between enterovirus 71 and its receptor SCARB2. Nature Microbiology, 4 (3). pp. 414-419. ISSN 2058-5276

https://doi.org/10.1038/s41564-018-0319-z

Structure of EV71 complexed with its receptor SCARB2 reveals an unexpected mode of engagement

Daming Zhou[1,*], Yuguang Zhao[1,*], Abhay Kotecha[1,5], Elizabeth E Fry[1], James Kelly[2], Xiangxi Wang[4], Zihe Rao[4], David J Rowlands[2], Jingshan Ren[1,†], David I Stuart[1,3,†]

[1] Division of Structural Biology, University of Oxford, The Henry Wellcome Building for Genomic Medicine, Headington, Oxford, OX3 7BN, UK.

[2] School of Molecular and Cellular Biology, Astbury Centre for Structural Molecular Biology, University of Leeds, Leeds, UK.

[3] Diamond Light Source Ltd, Harwell Science &Innovation Campus, Didcot, OX11 0DE, UK.

[4] National Laboratory of Macromolecules, Institute of Biophysics, Chinese Academy of Science, Beijing, 100101, China.

[5] Present Address: Materials and Structural Analysis, Thermo Fisher Scientific, Eindhoven, The Netherlands.

* These authors contributed equally to this work.

† Correspondences should be addressed to Jingshan Ren,phone: +44 1865 287545, e-mail: ren@strubi.ox.ac.uk or David I. Stuart, e-mail: dave@strubi.ox.ac.uk.

Enterovirus 71 (EV71) is a common cause of hand, foot and mouth disease (HFMD) a disease endemic especially in the Asia-Pacific region[1]. Scavenger receptor class B member 2 (SCARB2) is the major receptor of EV71, and several other enteroviruses responsible for HFMD, and plays a key role in cell entry[2]. Although the structures of EV71 and SCARB2 are known[3-6] we do not know how they interact to initiate infection. We report here the EV71-SCARB2 complex structure determined at 3.4 Å resolution using cryo-electron microscopy (cryoEM). This reveals that SCARB2 binds EV71 on the southern rim of the canyon, rather than across the canyon as was expected. Helices 152-163 and 183-193 of SCARB2 and the VP1 GH and VP2 EF loops of EV71 dominate the interaction, suggesting a plausible mechanism by which receptor binding might facilitate the low pH uncoating of the virus in the endo/lysosome. Remarkably, many residues within the binding footprint are not conserved across SCARB2 dependent enteroviruses, however a conserved proline and glycine seem key residues. Thus, although the virus maintains antigenic variability even within the receptor binding footprint, the identification of binding 'hotspots' may facilitate the design of receptor mimic therapeutics less likely to quickly generate resistance.

HFMD is a viral disease that infects mainly infants and children and has caused repeated epidemics in the Asia-Pacific region for more than 20 years[7], with around 2,000,000 cases every year since 2010. Whilst Coxsackievirus A16 (CV-A16) and EV71 are major etiological agents of HFMD, a variety of viruses in the genus Enterovirus, including many other type A and some type B enteroviruses also cause the disease[1]. HFMD usually leads to relatively mild symptoms, such as fever, oral ulcerations, and swellings on the hands and feet. However, EV71 infection is sometimes associated with cardiac and central nervous system complications and even death[8]. Enteroviruses belong to the picornavirus family of

icosahedral, unenveloped viruses[9]. They contain a positive sense single-stranded RNA genome which when released into the cytoplasm initiates infection, being directly translated by host ribosomes. This initial stages of infection involves attachment to a host cell protein receptor, internalisation, uncoating (which for enteroviruses is presumed to occur via expansion of the particle following ejection of a lipid pocket factor from the VP1 β-barrel resulting in a cascade of structural rearrangements[10]) and release of the genome through a membrane pore into the cytoplasm[11]. Correct engagement with a specific receptor is therefore critical to infectivity and can control virus tropism at both species and tissue level[12]. This makes receptor-virus interactions attractive targets for ant-viral therapeutics, since it may be more difficult for a virus to acquire resistance to such a compound than to a classic enzyme inhibitor. Recently, a number of receptors have been identified for many of the etiological agents of HFMDV, notable receptors include SCARB2 (a receptor for EV71, CV-A16 and a sub-group of type A enteroviruses)[2], Kremin1 for CV-A10[13], PSGL1 for EV71 and CAR and DAF for Group B enteroviruses[14]. The usage of receptors correlates with the capsid structure indicating that receptor switching drives evolution (Fig. 1a). Unfortunately to date there are no high resolution data available on receptor/HFDV complexes. It has however been inferred that SCARB2 binds at the so-called canyon, a depression that in enteroviruses encircles the icosahedral 5-fold axes and harbours the binding sites for slender immunoglobulin-domain based receptors [15], although SCARB2 is a much bulkier molecule.

SCARB2, also known as LIMP-2, is a type III membrane protein with N- and C-terminal transmembrane helices[16]. It is found especially in lysosomal limiting membranes and its 400 residue luminal domain is heavily glycosylated with nine potential N-linked glycosylation sites[6]. SCARB2 has a major role in endo/lysosomal membrane organization, with mutations causing several neurodegenerative and renal diseases. There is good evidence that attachment

to SCARB2 mediates internalisation and uncoating in EV71, and is required for the latter stages[17,18]. It has, however, been established that uncoating requires not only attachment to SCARB2, but also low pH. This implies that binding to SCARB2 might destabilise the virus particle at low pH (leading to the formation of expanded or 'A-particles'[5,10]). Our aim was to visualise the initial attachment complex and so we used a variant of EV71 genotype B2 whose infectivity is enhanced at low pH by a single mutation VP1 N104S (Methods). The particles were further stabilised by replacing the natural pocket factor by a potent expansion-inhibitor, NLD (Methods). Using these stabilised particles, we determined the structure of the luminal domain of SCARB2 in complex with EV71 at a pH of 5.1 by cryoEM (see Methods and Extended Data Fig. 1a). We find, unexpectedly, that SCARB2 binds to the 'southern rim' of the canyon, interacting with loops from two of the major capsid proteins, VP2 and VP1 (Fig. 1b). The structure is at sufficient resolution for us to build and refine an atomic model of the complex (Fig. 1c,d, Methods and Extended Data Table 1). The virus structure is in the un-expanded state with NLD remaining bound in the VP1 pocket (Fig. 1c) and the virus capsid is essentially indistinguishable from the native mature virus (the RMSD for 774 matched Cαs, out of a total of 784 is 0.4 Å). Interaction of the receptor with the virus is through helices α5 and α7, which together with α4 form a bundle lying distal from the domain termini, and therefore from the membrane (Fig. 2a)[6]. This is consistent with previous observations that the C-terminal end of α4 is directly involved in attachment and the observation that α5 forms part of the epitope of an Fab which binds SCARB2 to prevent virus attachment[19]. It has been noted that this helical bundle undergoes pH dependent conformational changes, and it has been proposed that these changes are involved in a pH dependent triggering of viral uncoating[3,6]. Interestingly, although our structural analysis was performed at relatively low pH (5.1) the structure of the helical bundle is essentially indistinguishable from that observed for the isolated protein at neutral pH[3,4,6] (Fig. 2b),

consistent with our strategy of locking the virus in a pre-uncoating state by using a mutant virus adapted to low pH and replacing the lipid pocket factor with the tighter binding NLD molecule (Methods). Whilst much of the surface of the luminal domain of SCARB2 is shielded by nine complex glycans the EV71 binding site is largely clear of glycosylation sites, although a long well-ordered phosphorylated sugar has been seen to approach this region of the SCARB2 surface[6] (Fig. 2a). Considering that it is highly exposed in the apo structure the binding site is surprisingly hydrophobic, suggesting that this region is involved in protein-protein interactions as part of its function in the host. Indeed it has been proposed that it's partner β-Glucosidase uses this region as part of its attachment site[6] (Extended Data Fig. 2c). In addition to hydrophobic interactions there are limited hydrogen bond and charge interactions which will be described below from the perspective of the virus. Overall the footprint of the receptor on the virus is ~700 $Å^2$, similar to that observed for tightly binding antibodies.

The SCARB2 binding site on EV71 is composed of residues from the VP2 EF and the VP1 GH loop, which form part of the south wall of the canyon and bear antigenic residues. The VP2 EF loop is shorter in EV71 than in most other enteroviruses (e.g. 15 residues shorter than for poliovirus type 1) and residues 134 to 162 from this loop, together with residues 214 to 216 in the VP1 GH loop form a platform upon which the receptor sits (Fig. 3a). The first hypothesis for receptor binding to enteroviruses (the canyon hypothesis, proposed in 1985) was that slender receptors would insert into the canyon, thereby allowing the necessarily conserved attachment residues to be concealed from immune surveillance, since the rather blunt antibody would be unable to reach into the canyon[20]. In the intervening years, it has become clear that across picornaviruses, receptor binding can be more varied (the current situation is summarized in Extended Data Fig. 3), however it remains true that this mode of

attachment is common amongst some enteroviruses (e.g. poliovirus). Indeed, the assumption has been that SCARB2 binding will follow this pattern[21] and so it is surprising that the binding site is essentially a platform that lies outside of the canyon, extending to the 'south' (Fig. 3b). This site is roughly similar to that observed for DAF binding to echovirus-7[22], and for integrin binding to foot-and-mouth disease virus [23], so that all current receptor attachment sites for picornaviruses can be grouped into three areas on the virus surface (Extended Data Fig. 3). The SCARB2 binding residues are unremarkable, largely non-conserved and there is no strong surface charge characterising the region (Fig. 3c,d). The interactions are detailed in Extended Data Table 2. In summary, there are 14 viral and 19 receptor residues involved in hydrophobic interactions (≤ 4.0 Å), 4 potential hydrogen bonds and 2 potential charged interactions. Of these, 3 of the key interactions are with the main chain of the viral polypeptides. A significant sub-set of the agents of HFMD use SCARB2 as a receptor (Fig. 1a) and it is likely that the binding site is conserved across these viruses. However a surprisingly large number of residues in the binding site are not conserved across the known SCARB2 binders (10 out of 14 residues, Extended Data Fig. 4). We assume that this variability arises from antigenic variation, which has presumably led to the differentiation of the SCARB2 binding subset of enteroviruses, indeed EV71 vaccine does not provide protection against another SCARB2 binding virus, CV-A16. How then do these viruses maintain specificity for SCARB2 in the face of sequence variation? Of the SCARB2 binding residues VP2 Gly 137, Pro 147 and Tyr 148 are conserved. From the antigenic perspective, only the tyrosine presents a signature side-chain recognition signal, but the others have structural properties that can control local protein folding. All three residues are involved in key interactions with SCARB2 (Fig. 3c,d). It appears that the recognition involves a significant proportion of side-chain independent interactions, which may mitigate the constraints imposed on antigenic variation by maintenance of receptor binding. A snapshot of

this can be seen in an analysis of the immune response of recovered patients[24], where by single cell sequencing, the epitopes of the key neutralising antibodies were mapped by identifying mutations in EV71 that abrogated neutralisation. The results are shown in Fig. 4a. It is striking that all except one of the mutations are outside of the SCARB2 footprint, scattered widely on the capsid, suggesting that neutralising responses are directed at epitopes that at most overlap the receptor binding site only partially. It appears that, rather akin to the exposed receptor binding site of foot-and-mouth disease virus[23], SCARB2 binding enteroviruses manage to hide their receptor binding site in full view of the immune response.

If the EV71/SCARB2 complex provides a counter example to the canyon hypothesis, does it clarify how receptor binding and low pH might trigger uncoating (for the canyon hypothesis receptor binding to the floor of the canyon could induce changes leading to the release of the pocket factor lying directly below the canyon floor). Fig. 4b shows the relative position of the SCARB2 attachment site, the pocket factor binding site, and the conformational changes that occur on transition to the expanded form of the virus and low pH form for SCARB2[3,4]. It seems plausible that in wild type virus, without additional stabilisation of the pocket, structural changes in the SCARB2 helical bundle induced as the pH drops (late endo/lysosome) would exert mechanical strain on the virus capsid. Specifically we find that SCARB2 attaches such that the pH induced conformational change observed previously would act as a lever on the VP1 GH loop through movement of α7 away from α5, which is strongly anchored to the VP2 EF loop. This agrees with our previous proposal that the VP1 GH loop, which undergoes conformational changes upon particle expansion, acts as the sensor in a sensor-adaptor uncoating mechanism[5,10,25], and initiates a cascade of changes, which include the loss/expulsion of the pocket factor and expansion of the particle to facilitate the release of the N-terminus of VP1, VP4 and, ultimately the viral genome. In

agreement with this we note that mutation of one of the VP1 GH loop residues (K215A) increases thermostability, but produces a slow growth phenotype[26]. This is an attractive mechanism, but remains speculative pending experimental evidence. Indeed some experimental results remain hard to explain, for instance mutation VP1 Q172A abolished binding to SCARB2 in pull-downs (and a similar result was seen with mutations of neighbouring residues), also VP1 mutations K98E, E145A and L169F enable EV71 to interact with murine SCARB2 [27,28] . It is conceivable that these residues, distant from the SCARB2 binding site, act through subtle allosteric affects. In summary, the complex of EV71 with SCARB2 reveals an unexpected mode of attachment, and suggests mechanisms of antigenic camouflage and receptor/pH mediated uncoating. Knowledge of the specific 'hot spots' of this interaction may help in the design of small molecules, or more likely biologics that block viral entry, for instance nanobodies, being smaller than antibodies, might be able to target residues that cannot be altered without compromising virus viability, indeed an unwitting proof of principle of this has been made by Xu et al.[29,30] who grafted parts of the VP1 GH and VP2 EF loops into a recombinant vaccine that protected mice from a lethal EV71 challenge.

Methods

Expression and Purification of SCARB2

Soluble truncated SCARB2 with His-tag was expressed in HEK 293T cells, as described earlier[6]. Cells were centrifuged at 1,500g for 20min and the supernatant was dialysed in buffer (1.7 mM NaH_2PO_4, 23 mM Na_2HPO_4, 250 mM NaCl, pH 8.0) at 4 °C for 48h. Then the sample was filtered and loaded to a 5mL HisTrap Nickel column (GE Healthcare). Buffer (20mM Tris, 200mM NaCl, 30mM immidazole, pH 8.0) was used to wash the Nickel column, followed by elution with buffer (20mM Tris, 200mM NaCl, 500mM imidazole, pH

8.0). Then the eluate was loaded onto a Superdex 75 16/60 gel filtration column (GE Healthcare) for further purification. Buffer (20mM Tris, 200mM NaCl, pH 8.0) was used for gel filtration. Purified SCARB2 was concentrated using a 10 KDa ultrafiltration tube (Amicon).

Virus Production and Purification

Low-pH-enhanced EV71 genotype B2, which has a mutation of VP1 N104S, was used to infect Vero cells[31]. 3 days after infection, virus was harvested and 0.5% (v/v) NP40 was added. The sample was stored at -80°C until needed. For purification, three freeze-thaw cycles were done to ensure full release of virus from the cells. Then 8% (w/v) PEG 6000 was added to precipitate virus. The sample was centrifuged at 3,500g for 1h at 4°C, then the pellet was suspended in ~35ml buffer (100mM Na-acetate, 200mM NaCl, 0.5% (v/v) NP40, pH 5.0) and centrifuged at 3,500g for 30 min at 4°C to remove cell debris. Virus particles in the supernatant were pelleted through a 2ml 30% (w/v) sucrose cushion (in 100mM Na-acetate, 200mM NaCl, pH 5.0) at 105,000g for 3h at 4°C. The pellet was suspended in buffer (100mM Na-acetate, 200mM NaCl, 0.5% (v/v) NP40, pH 5.0) and centrifuged at 12,000g for 30 min at 4°C to remove insoluble material. The supernatant was then laid on the top of a 15 - 45% sucrose gradient (in 100mM Na-acetate, 200mM NaCl, pH 5.0) and centrifuged at 105,000g for 3h at 4°C. Fractions containing EV71 full particles were harvested and sucrose in the sample was removed using a spin desalting column (Zeba, Pierce). Virus particles in buffer (100mM Na-acetate, 200mM NaCl, pH 5.0) were then concentrated using a 100 KDa ultrafiltration tube (Amicon).

Cryo-EM Sample Preparation

EV71 particles were incubated with EV71 inhibitor NLD[32,33] at 4°C for 24h, with a molar ratio of EV71 particle: NLD of 1:300. Then 0.5 μl of SCARB2 (6.5 mg/ml, in 20mM Tris,

200mM NaCl, pH 8.0) was mixed with 4.5 µl of EV71 (0.65mg/ml, in 100mM Na-acetate, 200mM NaCl, pH 5.0), with a molar ratio of EV71 particle: SCARB2 of 1:100. The pH of the mixture was 5.1. Immediately after this, the mixture was applied to a glow-charged ultrathin carbon grid (Agar Scientific), blotted by filter paper and vitrified by plunging into liquid ethane using a Vitrobot mark IV (FEI).

Cryo-EM Data Collection

Electron data were collected using a Tecnai F30 'Polara' microscope (FEI) operating at 300 kV, equipped with a Gatan GIF Quantum energy filter (30 eV energy selecting slit width) and a Gatan K2 Summit direct electron detector. Data was recorded as movies (32 frames, each 0.25 s) in super-resolution mode using SerialEM[34] with a defocus range 0.5 - 2.5 µm. The calibrated magnification was 37037x, corresponding to a pixel size of 1.35 Å. The dose rate was ~4 $e^-/ A^2/ s$, resulting in a total electron dose of 35 e^-/ A^2.

Cryo-EM Data Processing

Frames of each movie were aligned and averaged using MotionCorr2 [35] and the contrast transfer function parameters were determined with CTFFIND3[36]. Micrographs with astigmatism or significant drift were discarded. Particles were automatically picked using ETHAN[37] and then manually screened in EMAN2[38]. The structure was calculated with Relion 1.3 following the gold-standard refinement procedure[39]. Reference-free 2D-class averaging was performed for initial model generation. Template-based 3D classification and refinement was performed using initial models generated by filtering the crystal structure of EV71 (PDB: 3VBH[5]) to 50 Å resolution. The final density map was calculated using 10443 particles from 757 micrographs, with an overall resolution of 3.4 Å, estimated by Fourier shell correlation[39] (Extended Data Fig. 1a).

Model Building

The crystal structure of EV71 (PDB: 3VBH[5]) and the structure of SCARB2 (PDB: 4Q4B[6]) were fitted into the electric potential map in COOT[40]. The model was further improved using Phenix.real_space_refine[41]. VP1 residues 11-17 of EV71 were unclear and not built into the final model. Refinement statistics are given in Extended Data Table 1.

The residues forming the EV71-SCARB2 interface were identified with PISA [42]. The roadmaps were done using Rivem[43]. Coordinates 3J6N, 6EIT, 3J8F, 3DPR and 3IYP for virus-receptor complexes of CV-B3/CAR (Coxsackievirus and adenovirus receptor), CV-A24/ICAM-1, PV-1/CD155, HRV-2/V3 complex (very-low-density lipoprotein module V3) and echovirus-7/DAF (decay-accelerating factor) complex, respectively[15,22,44-47] were used for preparation of Extended Data Fig. 3. All figures were prepared with PYMOL [47] and CHIMERA[48].

Acknowledgments

D.Z. was supported by China Scholarship Council-University of Oxford Scholarship, J.R. by the Wellcome Trust (101122/Z/13/Z), and D.I.S. and E.E.F. by the UK Medical Research Council (MR/N00065X/1). This is a contribution from the UK Instruct Centre. The Wellcome Trust Centre for Human Genetics is supported by the Wellcome Trust (grant 090532/Z/09/Z).

Author Contributions

D.Z. and A.K performed experiments. D.Z., J.R., and D.I.S. analysed the results and together with E.E.F. and Y.Z. wrote the manuscript. All authors read and approved the manuscript.

Author Information

The structure is available from the PDB, accession code XXX. The electron density map is available from EMDB, accession code YYYY. The EM data are available from EMPIAR, accession code ZZZZ. Reprints and permissions information is available at www.nature.com/reprints. The authors declare competing financial interests: details are available in the online version of the paper. Readers are welcome to comment on the online version of the paper. Correspondence and requests for materials should be addressed to J.R. (ren@strubi.ox.ac.uk) or D.I.S. (dave@strubi.ox.ac.uk).

Figure Legends

Fig. 1 | Phylogeny and the quality of the EV71/SCARB2 EM structure. a, Phylogenetic tree of the HFMD causing enteroviruses derived by comparing the capsid sequences. **b**, EV71/SCARB2 complex viewed down the 2-fold icosahedral axis with left half of the particle shown as 3D reconstruction coloured by radius from blue through cyan, green and yellow to orange from lowest to highest radius, and right half of the complex shown as ribbons coloured in blue, green, red and orange for VP1, VP2, VP3 and SCARB2 respectively. **c**, **d**, Electron density maps for the bound pocket-binding inhibitor NLD and surrounding residues (**c**), and for residues at EV71 (green and blue lines) and SCARB2 (yellow lines) interface (**d**).

Fig. 2 | Complex formation of EV71 and SCARB2. a, The position and orientation of the bound SCARB2 on an EV71 protomer. EV71 VP1-4 are coloured in blue, green, red and yellow, respectively; the pocket-binding inhibitor NLD is shown as magenta spheres; VP1

GH and VP2 EF loops that interact directly with the receptor (orange ribbons) are drawn as thick coils. **b**, α4, α5 and α7 helix bundle of the EV71 bound SCARB2 (orange) has similar conformation to that of the apo structure at pH 6.5 (red). c, Conformational differences of the helix bundle of SCARB2 at pH 6.5 (red) and pH 4.8 (blue). The side chain of the putative pH sensor H150 that caps the C-terminus of α4 at pH 6.5 (red sticks) becomes the first residue of α5 at pH 4.8 (blue stick).

Fig. 3 | Details of EV71 and SCARB2 interactions. a, VP1 GH and VP2 EF loops form a platform for SCARB2 binding. The two loops and the receptor are shown as ribbons, and the rest of the viral protomer as surface representation. The colour scheme is as in the Fig. 2. **b**, Roadmap showing the foot print (brightly coloured) of SCARB2 on the viral surface. The black dots mark the canyon region of a viral protomer. **c**, Residues at the EV71 and SCARB2 interface. Side chains of EV71 are shown as cyan sticks, and those of SCARB2 as grey sticks. **d**, **e**, EV71 and SCARB2 interface with EV71 shown as an electrostatic surface and SCARB2 as sticks (**d**), and vice versa (**e**).

Fig. 4 | Epitopes of neutralizing antibodies and mechanism of uncoating. a, Roadmap showing the relative positions of the receptor foot print (bright blue and green) and escape mutations of neutralising antibodies (yellow). **b**, Cartoon representation showing the mechanism of receptor triggered uncoating of EV71. The α5 of the bound SCARB2 anchors the receptor on the binding platform consisting of the VP1 GH and VP2 EF loops. As the pH drops in the late endosome the pH sensor H150 triggers conformational changes of the helix bundle of α4, α5 and α7 of the receptor. α7 moves towards and distorts the conformation of the VP1 GH loop, which in turn triggers the release of the VP1 pocket factor and viral particle expansion.

References

1 Liu, S. L. *et al.* Comparative epidemiology and virology of fatal and nonfatal cases of hand, foot and mouth disease in mainland China from 2008 to 2014. *Reviews in medical virology* **25**, 115-128, doi:10.1002/rmv.1827 (2015).

2 Yamayoshi, S. *et al.* Scavenger receptor B2 is a cellular receptor for enterovirus 71. *Nature medicine* **15**, 798-801, doi:10.1038/nm.1992 (2009).

3 Dang, M. *et al.* Molecular mechanism of SCARB2-mediated attachment and uncoating of EV71. *Protein & Cell* **5**, 692-703, doi:10.1007/s13238-014-0087-3 (2014).

4 Neculai, D. *et al.* Structure of LIMP-2 provides functional insights with implications for SR-BI and CD36. *Nature* **504**, 172-176, doi:10.1038/nature12684 (2013).

5 Wang, X. *et al.* A sensor-adaptor mechanism for enterovirus uncoating from structures of EV71. *Nat Struct Mol Biol* **19**, 424-429, doi:10.1038/nsmb.2255 (2012).

6 Zhao, Y., Ren, J., Padilla-Parra, S., Fry, E. E. & Stuart, D. I. Lysosome sorting of β-glucocerebrosidase by LIMP-2 is targeted by the mannose 6-phosphate receptor. *Nature Communications* **5**, 4321, doi:10.1038/ncomms5321 (2014).

7 Wu, J. S. *et al.* Patterns of polymorphism and divergence in the VP1 gene of enterovirus 71 circulating in the Asia-Pacific region between 1994 and 2013. *Journal of virological methods* **193**, 713-728, doi:10.1016/j.jviromet.2013.07.051 (2013).

8 Jones, E. *et al.* Outcomes following severe hand foot and mouth disease: A systematic review and meta-analysis. *Eur J Paediatr Neurol*, doi:10.1016/j.ejpn.2018.04.007 (2018).

9 Pallansch, M. A. & Roos, R. *Enteroviruses: Polioviruses, coxsackieviruses, echoviruses, and newer enteroviruses*. (2007).

10 Ren, J. *et al.* Picornavirus uncoating intermediate captured in atomic detail. *Nat Commun* **4**, 1929, doi:10.1038/ncomms2889 (2013).

11 Tuthill, T. J., Groppelli, E., Hogle, J. M. & Rowlands, D. J. Picornaviruses. *Current topics in microbiology and immunology* **343**, 43-89, doi:10.1007/82_2010_37 (2010).

12 Ren, R. B., Costantini, F., Gorgacz, E. J., Lee, J. J. & Racaniello, V. R. Transgenic mice expressing a human poliovirus receptor: a new model for poliomyelitis. *Cell* **63**, 353-362 (1990).

13 Staring, J. *et al.* KREMEN1 Is a Host Entry Receptor for a Major Group of Enteroviruses. *Cell Host Microbe* **23**, 636-643 e635, doi:10.1016/j.chom.2018.03.019 (2018).

14 Baggen, J., Thibaut, H. J., Strating, J. & van Kuppeveld, F. J. M. The life cycle of non-polio enteroviruses and how to target it. *Nat Rev Microbiol* **16**, 368-381, doi:10.1038/s41579-018-0005-4 (2018).

15 Organtini, L. J., Makhov, A. M., Conway, J. F., Hafenstein, S. & Carson, S. D. Kinetic and structural analysis of coxsackievirus B3 receptor interactions and formation of the A-particle. *J Virol* **88**, 5755-5765, doi:10.1128/JVI.00299-14 (2014).

16 Calvo, D., Dopazo, J. & Vega, M. A. The CD36, CLA-1 (CD36L1), and LIMPII (CD36L2) gene family: cellular distribution, chromosomal location, and genetic evolution. *Genomics* **25**, 100-106 (1995).

17 Nishimura, Y. *et al.* Human P-selectin glycoprotein ligand-1 is a functional receptor for enterovirus 71. *Nature medicine* **15**, 794-797, doi:10.1038/nm.1961 (2009).

18 Yamayoshi, S., Ohka, S., Fujii, K. & Koike, S. Functional comparison of SCARB2 and PSGL1 as receptors for enterovirus 71. *J Virol* **87**, 3335-3347, doi:10.1128/JVI.02070-12 (2013).
19 Zhang, X. *et al.* The binding of a monoclonal antibody to the apical region of SCARB2 blocks EV71 infection. *Protein & Cell* **8**, 590-600, doi:10.1007/s13238-017-0405-7 (2017).
20 Rossmann, M. G. *et al.* Structure of a human common cold virus and functional relationship to other picornaviruses. *Nature* **317**, 145, doi:10.1038/317145a0 (1985).
21 Chen, P. *et al.* Molecular determinants of enterovirus 71 viral entry: cleft around GLN-172 on VP1 protein interacts with variable region on scavenge receptor B 2. *The Journal of biological chemistry* **287**, 6406-6420, doi:10.1074/jbc.M111.301622 (2012).
22 Plevka, P. *et al.* Interaction of decay-accelerating factor with echovirus 7. *J Virol* **84**, 12665-12674, doi:10.1128/JVI.00837-10 (2010).
23 Kotecha, A. *et al.* Rules of engagement between alphavbeta6 integrin and foot-and-mouth disease virus. *Nat Commun* **8**, 15408, doi:10.1038/ncomms15408 (2017).
24 Arthur Huang, K.-Y. *et al.* Epitope-associated and specificity-focused features of EV71-neutralizing antibody repertoires from plasmablasts of infected children. *Nature Communications* **8**, 762, doi:10.1038/s41467-017-00736-9 (2017).
25 Ren, J. *et al.* Structures of Coxsackievirus A16 Capsids with Native Antigenicity: Implications for Particle Expansion, Receptor Binding, and Immunogenicity. *J Virol* **89**, 10500-10511, doi:10.1128/JVI.01102-15 (2015).
26 Yuan, S. *et al.* Identification of Positively Charged Residues in Enterovirus 71 Capsid Protein VP1 Essential for Production of Infectious Particles. *Journal of Virology* **90**, 741-752, doi:10.1128/jvi.02482-15 (2016).
27 Chen, P. *et al.* Molecular determinants of enterovirus 71 viral entry: a cleft around Q172 on VP1 interacts with a variable region on scavenge receptor B 2. *Journal of Biological Chemistry*, doi:10.1074/jbc.M111.301622 (2012).
28 Victorio, C. B. L. *et al.* Cooperative effect of the VP1 amino acids 98E, 145A and 169F in the productive infection of mouse cell lines by enterovirus 71 (BS strain). *Emerging Microbes & Infections* **5**, e60-, doi:10.1038/emi.2016.56 (2016).
29 Xu, L. *et al.* Protection against Lethal Enterovirus 71 Challenge in Mice by a Recombinant Vaccine Candidate Containing a Broadly Cross-Neutralizing Epitope within the VP2 EF Loop. *Theranostics* **4**, 498-513, doi:10.7150/thno.7457 (2014).
30 Xu, L. *et al.* A Broadly Cross-protective Vaccine Presenting the Neighboring Epitopes within the VP1 GH Loop and VP2 EF Loop of Enterovirus 71. *Scientific Reports* **5**, 12973, doi:10.1038/srep12973 (2015).
31 Kelly, J. T. et al. Structural and functional characterization of an enterovirus 71 mutation that modulates receptor interactions *submitted* (2018).
32 De Colibus, L. *et al.* More powerful virus inhibitors from structure-based analysis of HEV71 capsid-binding molecules. *Nature structural & molecular biology* **21**, 282-288, doi:10.1038/nsmb.2769 (2014).
33 De Colibus, L. *et al.* Structure Elucidation of Coxsackievirus A16 in Complex with GPP3 Informs a Systematic Review of Highly Potent Capsid Binders to Enteroviruses. *PLoS Pathog* **11**, e1005165, doi:10.1371/journal.ppat.1005165 (2015).

34 Mastronarde, D. N. SerialEM: A Program for Automated Tilt Series Acquisition on Tecnai Microscopes Using Prediction of Specimen Position. *Microscopy and Microanalysis* **9**, 1182-1183, doi:10.1017/S1431927603445911 (2003).
35 Zheng, S. Q. *et al.* MotionCor2: anisotropic correction of beam-induced motion for improved cryo-electron microscopy. *Nature methods* **14**, 331-332, doi:10.1038/nmeth.4193 (2017).
36 Mindell, J. A. & Grigorieff, N. Accurate determination of local defocus and specimen tilt in electron microscopy. *Journal of structural biology* **142**, 334-347 (2003).
37 Kivioja, T., Ravantti, J., Verkhovsky, A., Ukkonen, E. & Bamford, D. Local average intensity-based method for identifying spherical particles in electron micrographs. *Journal of structural biology* **131**, 126-134, doi:10.1006/jsbi.2000.4279 (2000).
38 Tang, G. *et al.* EMAN2: an extensible image processing suite for electron microscopy. *Journal of structural biology* **157**, 38-46, doi:10.1016/j.jsb.2006.05.009 (2007).
39 Scheres, S. H. RELION: implementation of a Bayesian approach to cryo-EM structure determination. *Journal of structural biology* **180**, 519-530, doi:10.1016/j.jsb.2012.09.006 (2012).
40 Emsley, P. & Cowtan, K. Coot: model-building tools for molecular graphics. *Acta crystallographica. Section D, Biological crystallography* **60**, 2126-2132, doi:10.1107/s0907444904019158 (2004).
41 Afonine, P., Headd, J., Terwilliger, T. & Adams, P. New tool: phenix. real_space_refine. *Computational Crystallography Newsletter* **4**, 43-44 (2013).
42 Krissinel, E. & Henrick, K. Inference of macromolecular assemblies from crystalline state. *J Mol Biol* **372**, 774-797, doi:10.1016/j.jmb.2007.05.022 (2007).
43 Xiao, C. & Rossmann, M. G. Interpretation of electron density with stereographic roadmap projections. *Journal of structural biology* **158**, 182-187 (2007).
44 Baggen, J. *et al.* Role of enhanced receptor engagement in the evolution of a pandemic acute hemorrhagic conjunctivitis virus. *Proc Natl Acad Sci U S A* **115**, 397-402, doi:10.1073/pnas.1713284115 (2018).
45 Strauss, M. *et al.* Nectin-like interactions between poliovirus and its receptor trigger conformational changes associated with cell entry. *J Virol* **89**, 4143-4157, doi:10.1128/JVI.03101-14 (2015).
46 Querol-Audi, J. *et al.* Minor group human rhinovirus-receptor interactions: geometry of multimodular attachment and basis of recognition. *FEBS Lett* **583**, 235-240, doi:10.1016/j.febslet.2008.12.014 (2009).
47 DeLano, W. L. & Lam, J. W. PyMOL: A communications tool for computational models. *Abstr Pap Am Chem S* **230**, U1371-U1372 (2005).
48 Pettersen, E. F. *et al.* UCSF chimera - A visualization system for exploratory research and analysis. *J Comput Chem* **25**, 1605-1612, doi:10.1002/jcc.20084 (2004).

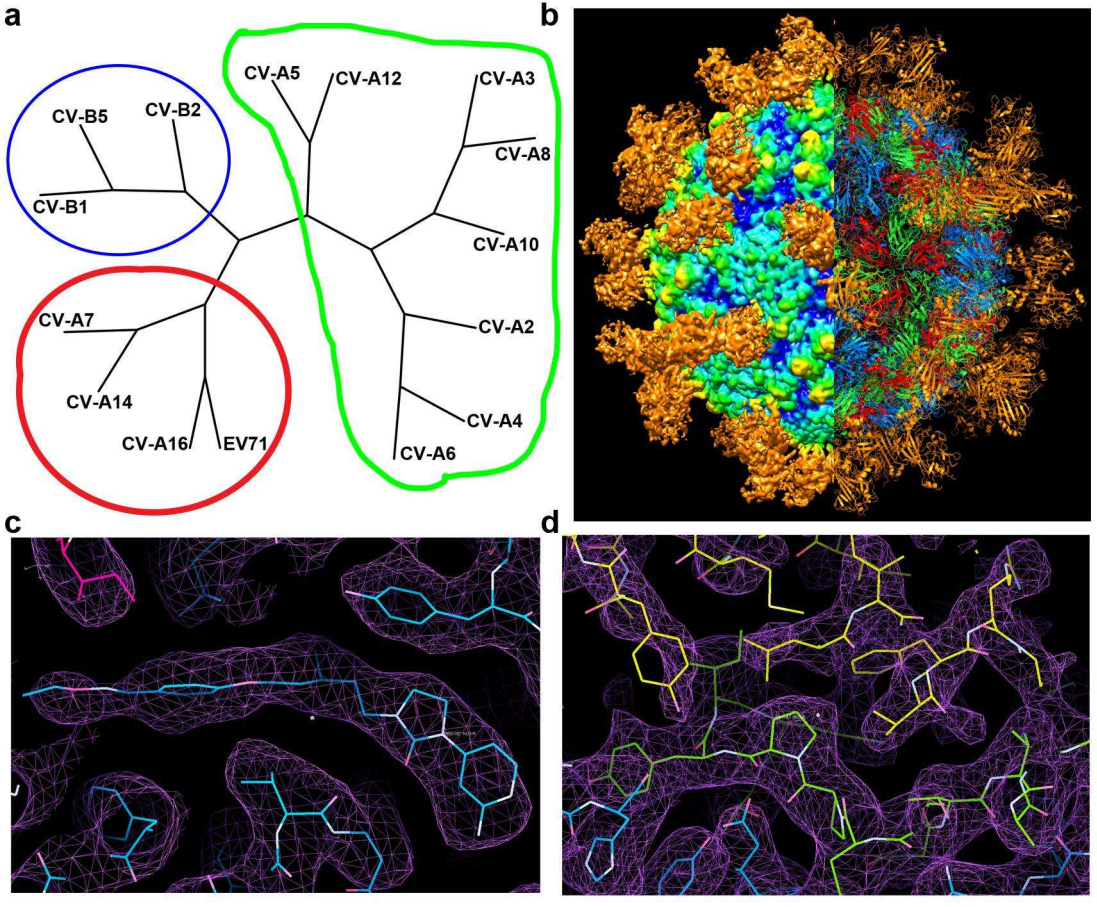
a
CV-A5
CV-A12
CV-A3
CV-B5
CV-B2
CV-A8
CV-B1
CV-A10
CV-A7
CV-A2
CV-A14
CV-A4
CV-A16
EV71
CV-A6
b
c
d

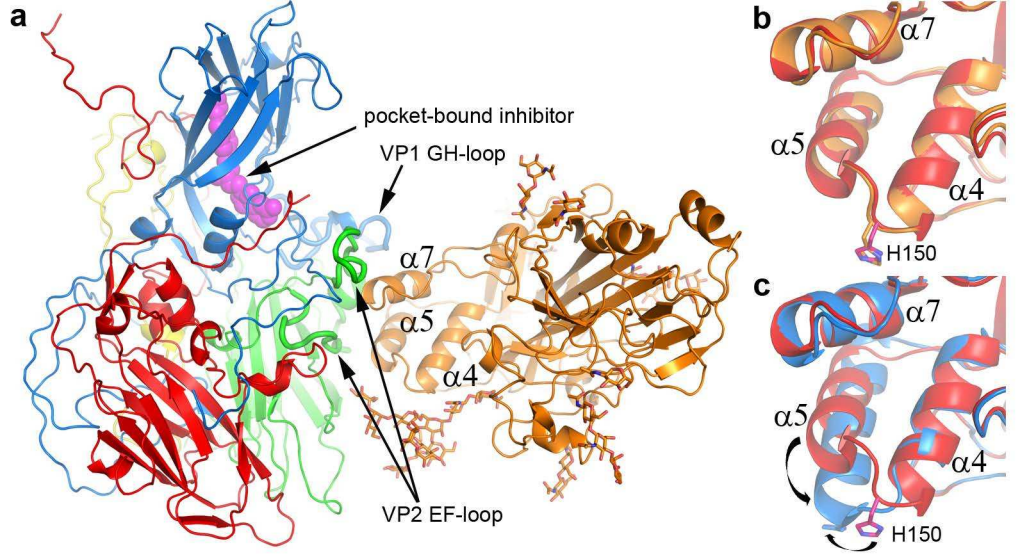
a
pocket-bound inhibitor
VP1 GH-loop
α7
α5
α4
VP2 EF-loop
b
α7
α5
α4
H150
c
α7
α5
α4
H150

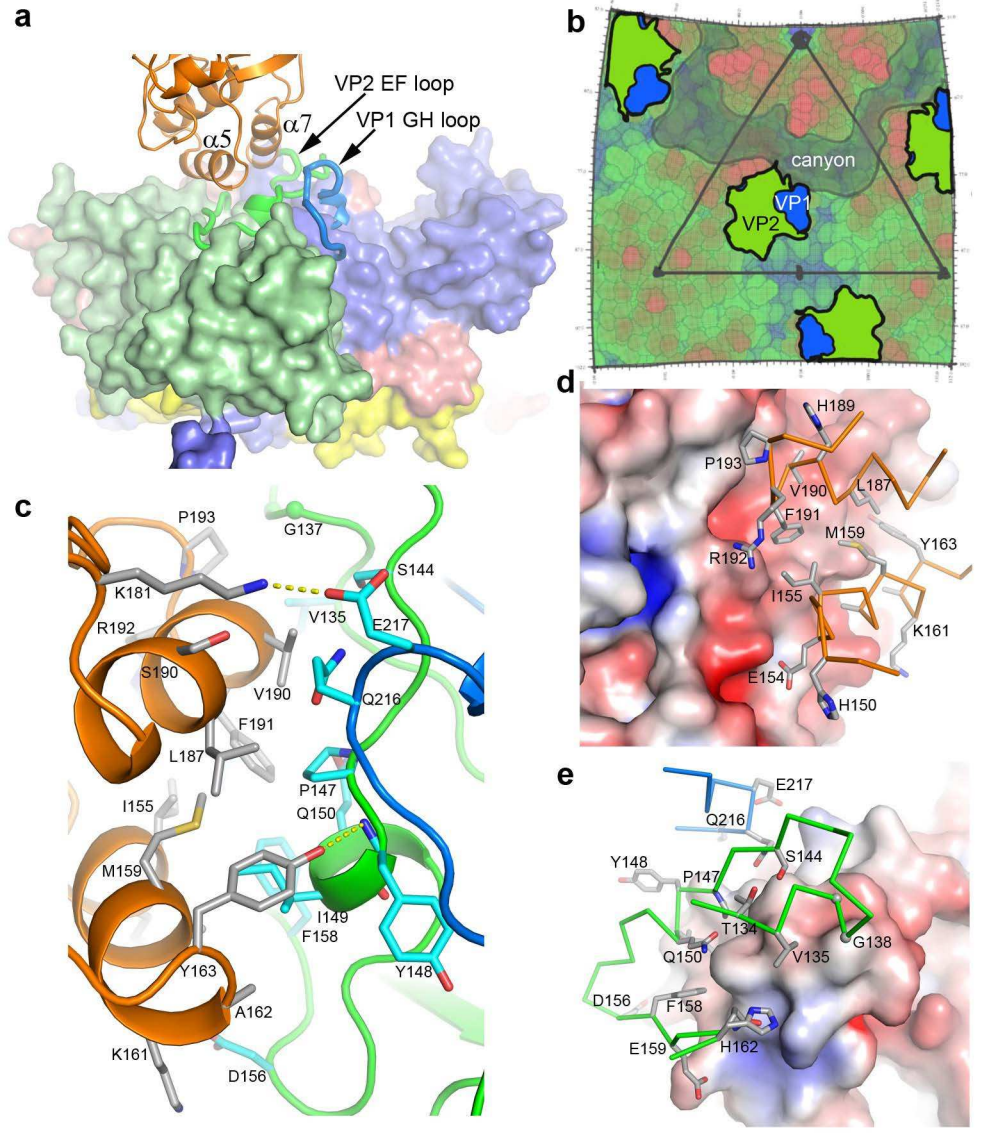
a
VP2 EF loop
VP1 GH loop
α5
α7
b
canyon
VP1
VP2
c
P193
G137
S144
K181
V135
E217
R192
S190
V190
Q216
F191
L187
P147
Q150
I155
M159
I149
F158
Y163
Y148
A162
K161
D156
d
H189
P193
V190
L187
F191
M159
Y163
R192
I155
K161
E154
H150
e
E217
Q216
Y148
P147
S144
T134
G138
Q150
V135
D156
F158
E159
H162

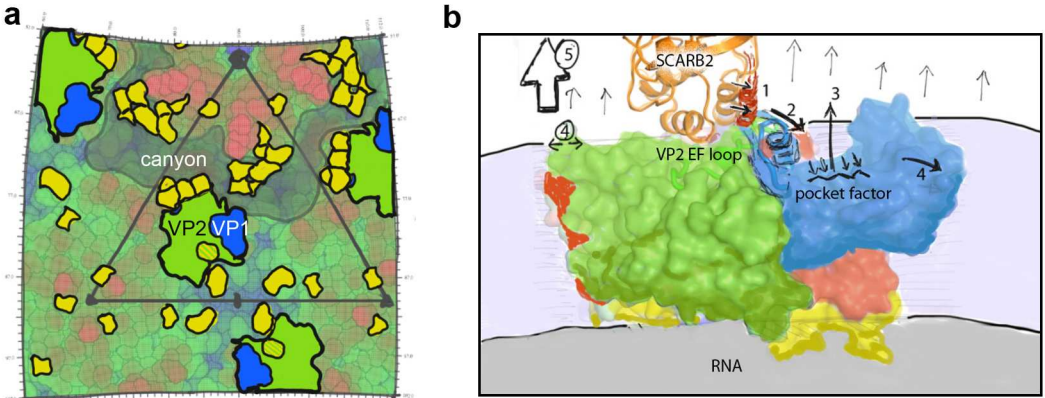
a
canyon
VP2
VP1
b
SCARB2
5
4
1
2
3
4
VP2 EF loop
pocket factor
RNA